Applied Acoustics 131 (2018) 112–128

Contents lists available at ScienceDirect

Applied Acoustics

journal homepage: www.elsevier.com/locate/apacoust

Technical note

Vibro-acoustics of a pipeline centrifugal compressor part I. Experimental study

Huihui Zhou[a], Yijun Mao[a,*], Qunlin Zhang[a], Cun Zhao[a], Datong Qi[a], Quan Diao[b]

[a] School of Energy and Power Engineering, Xi'an Jiaotong University, Xi'an, Shaanxi 710049, PR China
[b] Shenyang Blower Workgroup Co. Ltd, Shenyang, Liaoning 110869, PR China

ARTICLE INFO

Keywords:
Centrifugal compressor
Acoustic measurement
Tonal noise
Broadband noise
Coherence analysis

ABSTRACT

This paper presents an experimental study on the noise radiated from a centrifugal compressor unit, which mainly consists of a single-stage compressor connected with inlet and outlet pipes, a variable-frequency driving motor, a transmission gearbox and a bearing box. Sound pressure level spectra were measured at three rotational speeds each with several mass flow rates. The experimental results reveal that the overall sound pressure level increases with the rotational speed but varies slightly with the flow rate. The largest overall sound pressure level occurs at the measuring point near the motor, implying that the motor is one of the most important noise sources of the test rig. The frequencies of the tonal components are respectively consistent with the shaft frequency, the blade passing frequency of the compressor impeller and the interaction frequency of the magnetic flux wave with rotor slots in the variable-frequency motor. For sampling points near the connected pipes, the broadband noises mainly arise from the internal random pressure fluctuation through a curve fitting analysis of the squared sound pressure versus the dimensionless frequency. A coherence analysis between the acoustical and vibrational signals implies that the structural vibration induced by the internal pressure loads is the primary contributor for the compressor noise. Particularly, the outlet pipe with the highest vibration level should be a major concern for noise reduction of the centrifugal compressor.

1. Introduction

Fans and compressors are widely used in various engineering applications. Owing to the gas turbulence and its interaction with rotating blades and other boundaries, noise phenomena of these gas-conveying devices were studied over the past decades, aiming to reduce their negative effects on the device safety and the surroundings. Most of these investigations focused on the aerodynamic noise radiated from axial-flow fans and compressors in aero-engines owing to highly urgent demands on the reduction of airplane noise. The studies on this topic can be found in amounts of literature, such as [1–3].

Many researchers carried out extensive researches to clarify the noise mechanism and develop efficient noise control methods for centrifugal fans. For instance, Fehse and Neise [4] experimentally investigated the low frequency noise of a centrifugal fan and found that the low frequency noise of the centrifugal fan mainly arose from the flow separation on the shroud and the impeller blade suction sides. Velarde-Suarez et al. [5,6] experimentally identified the tonal noise source of the centrifugal fan, indicating that the volute tongue was the aerodynamic noise source. Mao et al. [7,8] and Cai et al.[9] employed the boundary element method to consider the scattering effect of the casing on sound radiation and scattering of a centrifugal fan. Based on the above understanding, some noise control methods have been developed to reduce the centrifugal fan noise, such as modification of the volute tongue [10] and metal foams coating on the volute tongue [11].

Some numerical and experimental studies were also carried out to clarify the aerodynamic noise mechanism of centrifugal compressors. Sun et al. [12] developed a numerical method using the FW-H equation to predict and optimize the aerodynamic noise of the impeller in the centrifugal compressor and the method was validated by the experimental data. Tang et al. [13] numerically identified the primary acoustic dipole source in the final stage of a multi-stage centrifugal compressor. Feld et al. [14] investigated the effects of the impeller and the influence of the inlet flow distortion on the noise in a high-speed centrifugal compressor. Ramakrishnan et al. [15] experimentally revealed the significant aero-acoustic excitation to the impeller at the vane passing frequency corresponding to the sum of the vane counts in the downstream vane rows. Ratior and Neise [16] conducted an experimental research to systematically reveal the sound generation mechanism in the centrifugal compressor. Broatch et al. [17] conducted an

* Corresponding author.
E-mail address: maoyijun@mail.xjtu.edu.cn (Y. Mao).

http://dx.doi.org/10.1016/j.apacoust.2017.10.011
Received 16 December 2016; Received in revised form 29 August 2017; Accepted 10 October 2017

Nomenclature

b_2	axial width of the impeller exit (mm)
c_{2r}	radial velocity at the impeller exit (m s^{-1})
D_{in}	inner diameter of the inlet pipe (mm)
D_1	mean diameter of the impeller inlet (mm)
D_2	mean diameter of the impeller exit (mm)
D_4	diffuser outlet diameter (mm)
D_{out}	outer diameter of the outlet pipe (mm)
$f_{BPF,2}$	blade passing frequency of the impeller of the compressor (Hz)
$f_{BPF,3}$	blade passing frequency of the cooling fan impeller mounted on the variable-frequency motor (Hz)
$f_{cooling}$	interaction frequency of the cooling air with the rotor slots of the variable-frequency motor (Hz)
f_{em}	frequency of the radial electromagnetic force wave of the variable-frequency motor (Hz)
f_g	gear meshing frequency (Hz)
$f_{n,1}$	shaft frequency of the variable-frequency motor (Hz)
$f_{n,2}$	shaft frequency of the centrifugal compressor (Hz)
n_1	rotational speed of the shaft of the variable-frequency motor (r min^{-1})
n_2	rotational speed of the impeller in the centrifugal compressor (r min^{-1})
n_3	rotational speed of the cooling fan impeller mounted on the variable-frequency motor (r min^{-1})
n_4	rotational speed of the main screwed pole in the oil pump (r min^{-1})
$\overline{P^2}$	squared sound pressure (Pa^2)
S_{xx}	power spectral density of the time signal x(t)
S_{yy}	power spectral density of the time signal y(t)
S_{xy}	cross power spectral density of the time signals x(t) and y (t)
u_2	circumferential velocity at the impeller exit (m s^{-1})
v^2	squared vibration velocity (m^2 s^{-2})
Z_1	rotor slots number of the variable-frequency motor
Z_2	impeller blade number of the centrifugal compressor
Z_3	impeller blade number of the cooling fan
Z_4	tooth number of the driven gear
β_{2A}	blade setting angle at the impeller outlet (degree)
δ_1	wall thickness of the inlet pipe (mm)
δ_2	wall thickness of the outlet pipe (mm)
ε	total pressure ratio
ω	circular frequency (Hz)
φ_{2r}	flow coefficient
γ^2	square magnitude of the coherence level

Abbreviation

BPF	blade passing frequency (Hz)
OASPL	overall A-weighted sound pressure level (dB)
SPL	sound pressure level (dB)

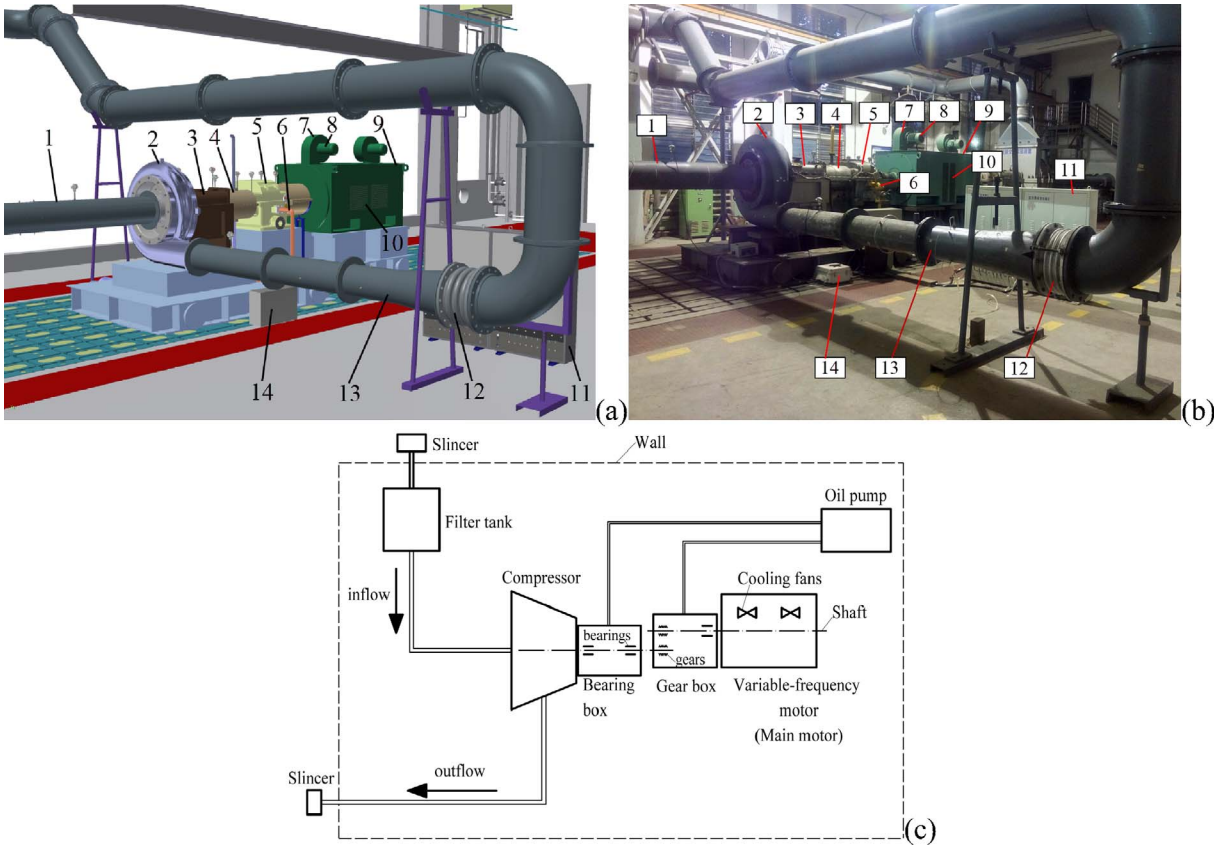

Fig. 1. Schematic of the experimental test rig: (a) The three-dimensional model; (b) The on-site view; (c) The schematic diagram. 1-inlet pipes, 2-centrifugal compressor, 3-bearing box, 4-coupling, 5-gear box, 6-lubricating oil lines, 7-cooling fan, 8-motor of the cooling fan, 9-variable-frequency motor (main motor), 10-cooling air vents, 11-pressure acquisition box, 12-expansion joint, 13-outlet pipes, 14- temperature acquisition box.